Available online at www.sciencedirect.com
SCIENCE DIRECT®
Biochemical and Biophysical Research Communications 310 (2003) 215–221
BBRC
www.elsevier.com/locate/ybbrc

Analysis of the stability of cytochrome c_6 with an improved stopped-flow protocol

Christian Lange, Manuel Hervás, and Miguel A. De la Rosa*

Instituto de Bioquímica Vegetal y Fotosíntesis, Centro de Investigaciones Científicas Isla de la Cartuja, Universidad de Sevilla y CSIC, Avda. Américo Vespucio s/n, 41092 Sevilla, Spain

Received 1 August 2003

Abstract

This work presents an improved stopped-flow protocol for the simultaneous measurement of thermodynamic and kinetic protein stability data from a single experiment, along with a formalism for the global analysis of the data. The method was applied to the comparison of the stabilities of cytochrome c_6 from *Anabaena* sp. PCC 7119 and one of its mutants (D72K). Compared to the wild type the mutant was found to have a significantly reduced thermodynamic ($\Delta\Delta G_{U0} = 2.7\,\mathrm{kJ\,mol^{-1}}$) and kinetic stability, as well as a more pronounced shift in transition state structure upon destabilization.

Keywords: Cytochrome c_6; Kinetic analysis; Protein folding; Protein stability; Stopped-flow; Urea-induced denaturation

Theoretical understanding of protein folding is advancing rapidly (for recent reviews, see e.g. [1,2]). However, for some time to come it will still be necessary to submit any theoretical model and any prediction to experimental tests. When mutant series are screened for the comparison of systematic predictions with real-world behavior it is desirable to have an experimental protocol available that allows for the rapid determination of kinetic and thermodynamic parameters of protein folding/unfolding transitions. Current protocols for the study of denaturant-dependent folding/unfolding either require expensive top-of-the-range stopped-flow instrumentation or tedious and time-consuming experimental manipulations, and separate kinetic and equilibrium experiments that consume large amounts of protein.

We present here an improved two-syringe stopped-flow protocol that allows the simultaneous measurement of thermodynamic and kinetic protein stability data from a single simple denaturant-dependent folding/unfolding experiment, along with a formalism for the global combined thermodynamic and kinetic analysis of the data. The method is applied to a comparison of the stabilities of the small heme protein cytochrome c_6 from the cyanobacterium *Anabaena* sp. PCC 7119 (cyt c_6) and one of its mutants (D72K). This mutant of the photosynthetic electron carrier cyt c_6 shows a significantly increased reactivity towards photosystem I [3], which made it interesting to assess the role of the mutation on the stability of the protein's structural framework.

Materials and methods

Expression and purification of proteins. Expression plasmids pEACwt and pEACD72K were kindly provided by Dr. Molina-Heredia [3,4]. Wild type cyt c_6 and D72K were expressed in *Escherichia coli* (strain GM119) that had been cotransfected with the plasmid pEC86 [5] (kindly provided by Dr. Thöny-Meyer, ETH, Zürich, Switzerland) and purified as described [3]. The purity of the protein preparations was greater than 95% as judged from the ratio of absorbance at 553 and 280 nm for reduced cyt c_6 and from the absence of other visible bands on Coomassie-stained SDS–PAGE. Protein concentrations were determined using an extinction coefficient ε_{553} of $26.2\,\mathrm{mM^{-1}\,cm^{-1}}$ [4] for reduced cyt c_6.

Circular dichroism spectra. Circular dichroism (CD) spectra were recorded with a MOS-450 AF/CD multi-purpose spectrophotometer (Bio-Logic SA, France) in a 1 mm quartz cuvette at 25 °C. Protein concentration was $40\,\mu\mathrm{g\,ml^{-1}}$ in 20 mM sodium phosphate buffer,

* Corresponding author. Fax: +34-954-460065.
E-mail address: marosa@us.es (M.A. De la Rosa).

0006-291X/$ - see front matter © 2003 Elsevier Inc. All rights reserved.
doi:10.1016/j.bbrc.2003.09.010

pH 7.0. The spectra were analyzed using the CDpro software package [6] with a 43-protein reference set (reference set 4).

Stopped-flow equipment. Stopped-flow experiments were carried out at 30 °C with a μSFM-20 device (BioLogic SA, France) fitted with a FC-15 cuvette and coupled to the MOS-450/AF-CD spectrometer. For fluorescence measurements, the instrument's photomultiplier tube was mounted at 90° with respect to the incident light and fitted with a Hoya U-360 band pass filter (Edmund Industrial Optics, NJ, USA). Excitation wavelength was 280 nm, except when CD kinetics were measured simultaneously, in which case it was 225 nm.

Equilibrium relaxation experiments. Solutions of 20 mM sodium phosphate, pH 7.0 (buffer), and 9.8 M urea in 20 mM sodium phosphate, pH 7.0 (buffered urea solution), both containing 50 μM potassium ferricyanide, were flushed with argon for 2 h. Equal volumes of concentrated (1–2 mM) oxidized cyt c_6 (wild type or D72K) were added to obtain equal concentrations (typically 1.0 μM) of native and unfolded protein. The solutions were transferred to the stopped-flow device and a series of shots was carried out in which varying ratios of native protein in buffer and unfolded protein in buffered urea solution (r) were mixed in a total volume of 560 μl with a total flow rate of 5.6 ml s^{-1}. Kinetic traces were recorded in duplicate or triplicate and averaged. Data were analyzed with Origin 5.0 (Jandel Scientific).

Chemicals. Urea was of SigmaUltra grade. All other chemicals were of at least analytical grade. All solutions were prepared with MilliQ water.

Results and discussion

Characterization of wild type cyt c_6 and D72K

Wild type cyt c_6 and D72K were successfully expressed in *E. coli* GM119 and purified to apparent homogeneity. The UV/VIS spectra as well as the redox potentials of wild type and mutant protein were virtually identical and our preparations were fully active as previously described [3]. To ensure that the introduction of the mutation had not grossly distorted the overall fold of cyt c_6, we recorded far-UV CD spectra. The spectra were very similar for wild type and D72K (not shown). When the fractions of secondary structure elements were calculated from the data, the contribution of regular α-helices was found to be $43 \pm 3\%$ for wild type cyt c_6 and $38 \pm 3\%$ for D72K. The fractions of all other secondary structure elements for wild type and D72K also coincided within the error margin. We conclude that the overall structure of cyt c_6 was not altered by the introduction of the D72K mutation except for a possible slight distortion of an α-helix.

Demonstration of two-state folding/unfolding transition

We chose to study the folding/unfolding transition of cyt c_6 by monitoring tryptophan fluorescence emission. This provides a very sensitive measurement of the mean distance between the heme and the single tryptophan residue (Trp 85) in the protein, and therefore the compactness of its structure [7]. However, fluorescence alone might not probe all phase transitions that occur upon folding/unfolding of a protein (see e.g. [8]). It was therefore necessary to employ an additional method. We observed the folding or unfolding of cyt c_6 simultaneously by tryptophan fluorescence emission and circular dichroism (CD) at 225 nm (Fig. 1). In both cases, CD and fluorescence kinetics seemed to match closely. The CD traces could be fit very well to single exponentials (Figs. 1A and C). The apparent rate constants (λ) obtained from these fits coincided with the ones obtained from the corresponding (fluorescence traces (Figs. 1B and D). For the shown experiments the λ values were 6.53 s^{-1} (CD) and 6.78 s^{-1} (fluorescence) for refolding (Figs. 1A and B) and 3.84 s^{-1} (CD) and 3.96 s^{-1} (fluorescence) for unfolding (Figs. 1C and D). Cyt c_6 does not contain additional histidines other than the fifth heme ligand His18 [4]. Alternative coordination of the heme group by additional histidines has been identified as the major source of kinetic heterogeneity in the folding/unfolding of *c*-type cytochromes [9–11], so in their absence monophasic and fully cooperative transitions were to be expected, and indeed this can be seen in the data. The unfolding transition of cyt c_6 can be described as a simple, reversible two-state transition $N \leftrightarrows U$ between its native state N and the unfolded state U, and can faithfully be probed by tryptophan fluorescence.

Setup of equilibrium relaxation experiments

To hold the concentration of protein constant while varying the concentration of denaturant in a two-syringe stopped-flow system, without losing ease and speed of handling, we introduced an experimental protocol in which equal concentrations of protein in buffer and in a solution of denaturant (in this case urea) were mixed in varying ratios. After mixing, this creates a situation parallel to relaxation experiments like *T*-jump or *p*-jump experiments where the concentrations of folded and unfolded protein are disturbed from and subsequently relax to their corresponding equilibrium values with a characteristic rate constant (for examples for the application of fast relaxation techniques to protein folding see [12–16]). Observing the relaxation of the disturbed equilibrium over a range of denaturant concentrations potentially yields data that contain the complete thermodynamic and kinetic information of a folding/unfolding transition, limited only by the time resolution of the stopped-flow instrument. The results of two typical experiments with wild type cyt c_6 and D72K are shown in Figs. 2A and B. The folding/unfolding reaction reached equilibrium on a sub-second timescale. By reading out the fluorescence intensities at equilibrium (F_{eq}) we obtained equilibrium stability curves as the ones represented in Figs. 2C and D. The mutant D72K was far less resistant to urea-induced unfolding (transition midpoint $[\text{urea}]_{50} = 3.56 \pm 0.09$ M) than the wild type ($[\text{urea}]_{50} = 6.06 \pm 0.15$ M). The data were analyzed assuming a simple two-state transition and a linear

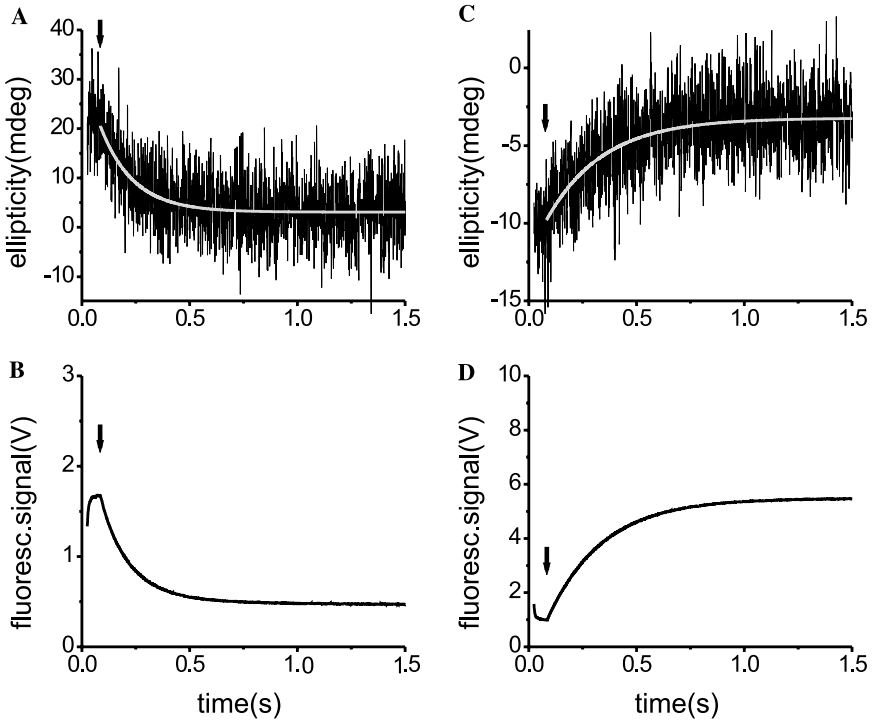

Fig. 1. Folding and unfolding kinetics of wild type cyt c_6. For refolding, cyt c_6 in a buffered solution of 8.6 M urea was mixed with 9 volumes of a buffered solution of 3.6 M urea (A,B). For unfolding, cyt c_6 in buffer was mixed with 9 volumes of a buffered solution of 9.8 M urea (C,D).The kinetics were monitored simultaneously by CD at 225 nm (A,C) and tryptophan fluorescence emission (B,D). Light lines in (A,C) represent single exponentials fit to the data (see text). Final concentration of cyt c_6 was 20 μM. Arrows indicate flow stop. Data are averages of 10 consecutive stopped-flow traces.

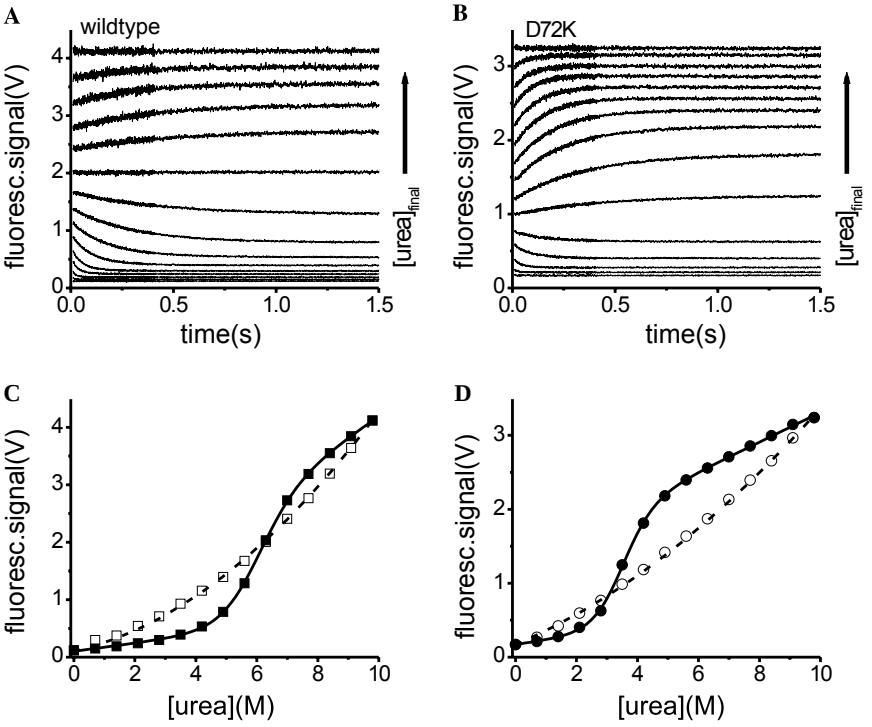

Fig. 2. Folding equilibrium relaxation experiments for wild type cyt c_6 (A) and D72K (B). Arrows on the right indicate increasing $[\text{urea}]_{\text{final}}$ (0–9.8 M). Equilibrium fluorescence signals (F_{eq}) (filled symbols) and initial fluorescence signals (F_{t0}) (open symbols) from the experiments shown in (A,B) are plotted as a function of [urea] in (C,D). Solid lines represent a fit of Eq. (3) to the F_{eq} values. The $\Phi_{N0,U0}$ and $\mu_{U,N}$ values obtained from this fit were used to calculate expected values for F_{t0} (dashed lines) according to Eq. (4).

dependency of the free enthalpy for unfolding (ΔG_U) on the urea concentration ([urea])

$$\Delta G_U = \Delta G_{U0} + m_{eq} \cdot [\text{urea}] \quad (1)$$

with ΔG_U at 0 [urea], ΔG_{U0}, and the denaturant interaction parameter m_{eq}. Equally linear dependencies of the intrinsic fluorescence intensities ($\Phi_{N,U}$)

$$\Phi_{N,U} = \Phi_{N0,U0} + \mu_{N,U} \cdot [\text{urea}] \quad (2)$$

were assumed for the native and unfolded protein; $\Phi_{N0,U0}$ represents $\Phi_{N,U}$ at 0 [urea], while $\mu_{N,U}$ describes the corresponding urea dependencies. The equilibrium fluorescence intensities (F_{eq}) are then given by

$$F_{eq} = \left(\Phi_N + \Phi_U \cdot e^{\Delta G_U/-RT}\right)/\left(1 + e^{\Delta G_U/-RT}\right). \quad (3)$$

Thus, ΔG_{U0} and m_{eq} can be obtained from the measured F_{eq} values by non-linear curve fitting. With this method we found D72K ($\Delta G_{U0} = 18.0 \pm 1.0\,\text{kJ mol}^{-1}$) to be $2.8\,\text{kJ mol}^{-1}$ less stable than the wild type ($\Delta G_{U0} = 20.8 \pm 1.4\,\text{kJ mol}^{-1}$). The urea interaction parameter (m_{eq}) was considerably greater for D72K ($-5.06\,\text{kJ mol}^{-1}\,\text{M}^{-1}$) than for the wild type ($-3.44\,\text{kJ mol}^{-1}\,\text{M}^{-1}$). This effect is responsible for the major part of the observed loss of apparent stability of D72K against denaturation by urea (see above), while the observed reduction in ΔG_{U0} plays a smaller role. The high m_{eq} value indicates a larger difference in solvent-accessible area upon unfolding for D72K as compared to the wild type [17]. This might be explained by a reduced compactness of the unfolded protein in D72K due to increased electrostatic repulsion. However, carrying out the folding/unfolding experiment in the presence of 100 mM NaCl did not significantly reduce m_{eq} (not shown). A possible interpretation for this may be that a local perturbation caused by the mutation reduces the propensity for formation of the C-terminal helix in the unfolded ensemble of states.

Absence of fast phase

In many studies of protein folding, loss of signal amplitude within the experimental dead times has been observed and ascribed to a fast collapse of the unfolded into an intermediate state (e.g. [18–21], but see [22]). Before attempting an analysis of the observed folding/unfolding of cyt c_6, it was therefore crucial to establish that no kinetic information was lost to these so-called "burst phases." When the kinetic traces for any one of our experiments were fit individually with single exponentials, the observed kinetic amplitude (A_F) and the equilibrium response signal (F_{eq}) at any given [urea] would add up to a value F_{t0} very close to the one predicted from the fluorescence parameters obtained by a fit of Eq. (3) to the equilibrium responses, according to

$$F_{t0} = A_F + F_{eq} = (1 - r) \cdot \Phi_N + r \cdot \Phi_U \quad (4)$$

for any given mixing ratio (r). This is shown for two experiments in Figs. 2C and D. We conclude that the observed kinetics contain the complete information and no amplitude is lost to reactions hidden within the dead time.

Data analysis

Apart from the stability data that can be extracted from an equilibrium analysis, we were interested in obtaining a meaningful set of parameters for comparison of the kinetic stability of cyt c_6 and its mutant. Analysis of the folding/unfolding kinetics based on fitting of the individual experimental curves proved unsatisfactory. The level of experimental variability was relatively high. We therefore chose to fit our experimental data globally, i.e., all traces from one experiment were fit simultaneously to a set of equations with common parameters. The global analysis of data provides for a stringent test of proposed models for protein folding/unfolding [23,24]. The ability of a given model to accurately fit the entirety of the data may be judged more convincingly, while at the same time more data points enter into the fitting. Consequently, the effect of experimental variability on the results will be reduced and their overall reliability increased. For the analysis of our experimental data, Eqs. (1) and (2) were assumed to hold throughout (for an account of the basis for these assumptions, see e.g. [25,26]). Kinetic protein unfolding data have been widely analyzed assuming a linear dependency of the activation energies ($\Delta G_{N-\ddagger}$ and $\Delta G_{U-\ddagger}$) on [urea]. In such a case the microscopic unfolding rate constant (k_U) is given by

$$\ln k_U = \ln k_{U0} - \frac{1}{RT} \cdot m_{k1} \cdot [\text{urea}] \quad (5)$$

with k_{U0} being k_U at 0 [urea]. The urea dependency of $\Delta G_{N-\ddagger}$ is expressed by m_{k1}. This is referred to as the "linear model" in this paper. The apparent rate constant (λ) for a two-state transition is given by the sum of k_U and the reverse (folding) rate constant (k_F). For the global analysis of our experimental data k_F was expressed in terms of k_U and ΔG_U, exploiting the fundamental link between kinetics and thermodynamics:

$$\lambda = k_U + k_F = k_U \cdot \left(1 + e^{\Delta G_U/RT}\right). \quad (6)$$

This reduces the number of fitting parameters, and that this be possible and give rise to a reasonable fit is one of the key tests for the applicability of a simple $N \leftrightarrows U$ reaction scheme. The "linear" model, although giving satisfactory global fits (see below), was not able to account for all aspects of our data. The λ values from individual fits of the kinetic traces would not produce the expected "V"-shaped Chevron plots (Figs. 3A and B). Deviations were most clearly observed for D72K at high [urea] (Fig. 3B), but both "roll over" at low [urea]

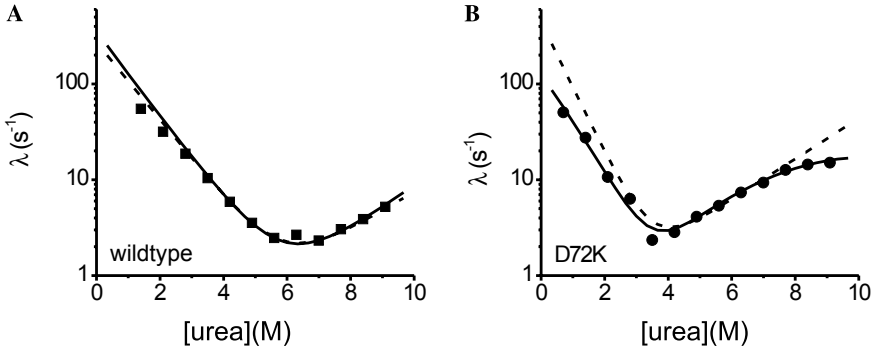

Fig. 3. Apparent rate constants λ for the urea-induced folding/unfolding of wild type cyt c_6 (A) and D72K (B). Lines represent values for λ calculated from global fits to the experimental data according to the "linear" (dashed lines) and "square term" (solid lines) models.

and "roll down" at high [urea] could also be identified in the Chevron plots of the wild type data (Fig. 3A). Additional parameters had to be introduced for a more accurate description of the cyt c_6 folding/unfolding transition. The most straightforward way to do this is to introduce a square term into the dependence of the activation energy $\Delta G_{N-\ddagger}$ on [urea], leading to the "square term" model. The urea dependency of k_U then reads

$$\ln k_U = \ln k_{U0} - \frac{1}{RT} \cdot \left(m_{k1}[\text{urea}] + m_{k2}[\text{urea}]^2 \right), \qquad (7)$$

while Eqs. (1) and (6) still hold. The newly introduced parameter (m_{k2}) may be interpreted as a measure of Hammond-type [27] changes in the transition state (‡) with increasing [urea] (see below).

Fitting results

For comparison, we fit our data sets with both the "linear" and the "square term" models. The goodness of fit as expressed by the χ^2 values calculated by the fitting algorithm was not dramatically different for the two methods. For wild type cyt c_6 the χ^2 values for the "square term" model were $101 \pm 14\%$ ($n = 4$) of those for the "linear" model. For D72K the "square term" model gave significantly superior fits. The χ^2 values were on average $86.3 \pm 9.1\%$ ($n = 3$) of those obtained with the "linear" model. An important criterion for the quality of fitting methods is their ability to reproduce detailed aspects of the data. Figs. 3A and B represent the apparent rate constants (λ) obtained from individual fits of the kinetic traces of two relaxation experiments with wild type cyt c_6 and D72K, along with the values calculated from the corresponding global fits. For the wild type an unambiguous choice between the two models could not be made based on the agreement between the calculated and the experimentally determined λ values (Fig. 3A). For D72K however, the "square term" model produced a far superior agreement (Fig. 3B). To gain an additional criterion we performed autocorrelation analysis of residuals (data not shown), which showed that phase shifts between the experimental and the fitted kinetic traces for both wild type cyt c_6 and D72K were clearly reduced with the "square term" model. We conclude that this model provides an accurate fit of the data and represents a valid working model for the characterization of the kinetics and thermodynamics of the folding/unfolding transition in cyt c_6. The final results of the global analysis with this model are summarized in Table 1. The results of the analysis with the "linear" model are included in the table for comparison, but will not be discussed further. Similar to the results from the analysis of the equilibrium fluorescence signals (see above), the stability of D72K was found to be reduced by $2.7\,\text{kJ mol}^{-1}$ compared to the wild type, and the absolute value of the urea interaction parameter (m_{eq}) was considerably greater for this mutant ($-3.60\,\text{kJ mol}^{-1}\,\text{M}^{-1}$ for wild type and

Table 1
Results of the global fits to the equilibrium relaxation experiments*

	ΔG_{U0} (kJ mol^{-1})	m_{eq} (kJ mol^{-1} M^{-1})	$\log k_{U0}$ (s^{-1})	m_{k1} (kJ mol^{-1} M^{-1})	m_{k2} (kJ mol^{-1} M^{-2})
"Linear" model					
Wild type	22.0 ± 1.4	-3.70 ± 0.20	-1.40 ± 0.27	-1.41 ± 0.25	–
D72K	18.07 ± 0.34	-5.03 ± 0.15	-0.513 ± 0.063	-1.248 ± 0.073	–
"Square term" model					
Wild type	21.4 ± 1.3	-3.60 ± 0.22	-1.45 ± 0.53	-1.74 ± 0.86	0.027 ± 0.063
D72K	18.67 ± 0.27	-5.21 ± 0.17	-1.096 ± 0.053	-2.51 ± 0.19	0.113 ± 0.022

* All values are means of 4 (wild type) and 3 (D72K) experiments ± SD.

$-5.21\,\mathrm{kJ\,mol^{-1}\,M^{-1}}$ for D72K). The loss in thermodynamic stability was accompanied by a loss in kinetic stability. The mean unfolding rate constant at 0 [urea] (k_{U0}) was $0.035\,\mathrm{s^{-1}}$ for the wild type, while it was increased to $0.080\,\mathrm{s^{-1}}$ for D72K. The m_{k1} value, which mainly expresses the increase in k_U with [urea], was $-1.74\,\mathrm{kJ\,mol^{-1}\,M^{-1}}$ for the wild type and $-2.51\,\mathrm{kJ\,mol^{-1}\,M^{-1}}$ for D72K, indicating a greatly increased influence of urea on the kinetic stability of the mutant.

Absence of kinetic intermediates

As an alternative kinetic model that would potentially yield more detailed information about the pathway of cyt c_6 folding/unfolding we applied the formalism laid out by Bachmann and Kiefhaber [28], who explained the "roll down" in the Chevron plot of their tendamistat unfolding data in terms of a non-populating on-pathway intermediate. In our case, the global fits of this model (not shown) were of good quality. However, the obtained numerical values of the microscopic rate constants would indicate an intermediate state whose free enthalpy lies in between the N and U states under certain conditions. This is in contradiction to the assumptions defining the model and in disagreement with the observed monophasic kinetics. This model therefore cannot describe the folding/unfolding of cyt c_6. Any other kinetic model containing intermediate states would necessarily lead to more complex multiphase kinetics. We conclude that the folding/unfolding of cyt c_6 proceeds by a pathway that does not contain any appreciable local energy minima, or intermediate states.

α value analysis

When a protein folding/unfolding transition is analyzed based on the assumption of a linear dependency of $\ln k_U$ on [urea], the α value, defined as

$$\alpha = \frac{m_{\mathrm{eq}} - m_{k1}}{m_{\mathrm{eq}}}, \tag{8}$$

can be taken as a measure of native-like structure in the transition state [17]. Whereas $\alpha = 1$ would indicate an all native-like transition state, $\alpha = 0$ would indicate an all unfolded-like one. For most proteins that show two-state folding behavior, α lies between 0.6 and 0.9 [29]. Using the results from the "linear" model (Table 1) we obtained α values of 0.62 for wild type cyt c_6 and 0.75 for D72K, indicating a more native-like transition state for the mutant. This however was unsatisfactory due to the inability of this model to accurately describe the kinetics of the system (see above). After realizing that the above definition of α corresponds to $\alpha = -\mathrm{d}\ln k_F / \mathrm{d}\ln K_U$ (K_U being the unfolding equilibrium constant), it is possible to apply this measure to any function for the dependency of $\ln k_F$ (and $\ln K_U$) on [urea]. For the "square term" model, we straightforwardly get

$$\alpha = \frac{m_{\mathrm{eq}} - (m_{k1} + 2 \cdot m_{k2} \cdot [\mathrm{urea}])}{m_{\mathrm{eq}}}. \tag{9}$$

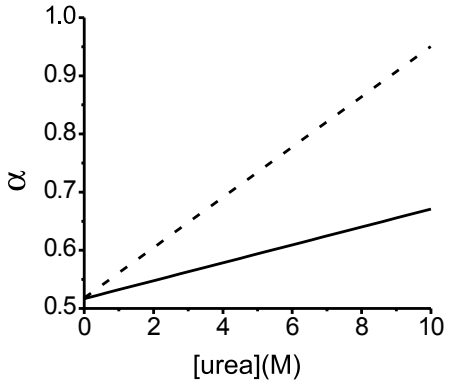

Fig. 4. α values for the folding/unfolding transition of wild type cyt c_6 (solid line) and D72K (dashed line) calculated according to Eq. (9).

The results of this analysis for the folding/unfolding of wild type cyt c_6 and D72K are shown in Fig. 4. For both proteins, α increases with increasing [urea]. This corresponds to a shift of the transition state towards a more native-like structure upon destabilization, as predicted by the Hammond principle [27]. The effect is far more pronounced for the mutant, in agreement with its reduced kinetic stability. Shifting transition states in protein unfolding have been reported and described in some detail before (see e.g. [30–32]). The advantage of the α-value analysis as presented here lies in the relative simplicity with which it parameterizes the denaturant-dependent shift in transition state.

Conclusions

Protein stability studies, especially when carried out on larger series of proteins, require an experimental approach that allows for the rapid assessment of kinetic and thermodynamic parameters of a protein's folding/unfolding transition, ideally from a fast, single experiment. The experimental protocol presented here fulfills these requirements. After the reversibility of a folding/unfolding transition has been assured, the equilibrium relaxation experiment can be carried out and within a short time provide a wealth of data that in principle contains the complete kinetic and thermodynamic information for the studied transition. The applied global method of analysis allows parameterizing this information in a straightforward way ideally suited for the purpose of comparisons between mutants or any homologous proteins.

Acknowledgments

This work was supported by the Spanish Ministry of Science and Technology (MCYT Grant BMC 2000-444) and the Andalusian Government (PAI, CVI-198). C.L. received a fellowship from the European Union's Research Training Network program (HRPN-CT-1999-00095). We thank Dr. José A. Navarro for helpful discussions and Dr. Javier Sancho for his critical comments on the manuscript.

References

[1] V. Daggett, A.R. Fersht, Is there a unifying mechanism for protein folding?, Trends Biochem. Sci. 28 (2003) 18–25.
[2] T. Head-Gordon, S. Brown, Minimalist models for protein folding and design, Curr. Opin. Struct. Biol. 13 (2003) 160–167.
[3] F.P. Molina-Heredia, A. Díaz-Quintana, M. Hervás, J.A. Navarro, M.A. De la Rosa, Site-directed mutagenesis of cytochrome c_6 from *Anabaena* species PCC 7119, J. Biol. Chem. 274 (1999) 33565–33570.
[4] F.P. Molina-Heredia, M. Hervás, J.A. Navarro, M.A. De la Rosa, Cloning and correct expression in *Escherichia coli* of the *pet*E and *pet*J genes respectively encoding plastocyanin and cytochrome c_6 from the cyanobacterium *Anabaena* sp. PCC7119, Biochem. Biophys. Res. Commun. 243 (1998) 302–306.
[5] E. Arslan, H. Schulz, R. Zufferey, P. Künzler, L. Thöny-Meyer, Overproduction of the *Bradyrhizobium japonicum c*-type cytochrome subunits of the cbb_3 oxidase in *Escherichia coli*, Biochem. Biophys. Res. Commun. 251 (1998) 744–747.
[6] N. Sreerama, R.W. Woody, Estimation of protein secondary structure from CD spectra: comparison of CONTIN, SELCON and CDSSTR methods with an expanded reference set, Anal. Biochem. 282 (2000) 252–260.
[7] T.E. Huntley, P. Strittmatter, The effect of heme binding on the tryptophan residue and the protein conformation of cytochrome b_5, J. Biol. Chem. 247 (1972) 4641–4647.
[8] J. Shimada, E.I. Shakhnovich, The ensemble folding kinetics of protein G from an all-atom Monte Carlo simulation, Proc. Natl. Acad. Sci. USA 99 (2002) 11175–11180.
[9] H. Roder, G.A. Elöve, W. Englander, Structural characterization of folding intermediates in cytochrome *c* by H-exchange labeling and proton NMR, Nature 335 (1988) 700–704.
[10] M.M. Pierce, B.T. Nall, Coupled kinetic traps in cytochrome *c* folding: His-heme misligation and proline isomerization, J. Mol. Biol. 298 (2000) 955–969.
[11] S.J. Hagen, R.F. Latypov, D.A. Dolgikh, H. Roder, Rapid intrachain binding of histidine-26 and histidine-33 to heme in unfolded ferricytochrome *c*, Biochemistry 41 (2002) 1372–1380.
[12] G.J. Vidugiris, J.L. Markley, C.A. Royer, Evidence for a molten globule-like transition state in protein folding from determination of activation volumes, Biochemistry 34 (1995) 4909–4912.
[13] R. Gilmanshin, S. Williams, R.H. Callender, W.H. Woodruff, B.R. Dyer, Fast events in protein folding: relaxation dynamics of secondary and tertiary structure in native apomyoglobin, Proc. Natl. Acad. Sci. USA 94 (1997) 3709–3713.
[14] J.C. Lee, H.B. Gray, J.R. Winkler, Cytochrome c' folding triggered by electron transfer: fast and slow formation of four-helix bundles, Proc. Natl. Acad. Sci. USA 98 (2001) 7760–7764.
[15] M.H. Jacob, C. Saudan, G. Holtermann, A. Martin, D. Perl, A.E. Merbach, F.X. Schmid, Water contributes actively to the rapid crossing of a protein unfolding barrier, J. Mol. Biol. 318 (2002) 837–845.
[16] C.-R. Rabl, S.R. Martin, E. Neumann, P.M. Bayley, Temperature jump kinetic study of the stability of apo-calmodulin, Biophys. Chem. 101–102 (2002) 553–564.
[17] C. Tanford, Protein denaturation. C. Theoretical models for the mechanism of denaturation, Adv. Protein Chem. 24 (1970) 1–95.
[18] W.A. Houry, D.M. Rothwarf, H.A. Scheraga, Circular dichroism evidence for the presence of burst-phase intermediates on the conformational folding pathway of ribonuclease a, Biochemistry 35 (1996) 10125–10133.
[19] M.C. Shastry, H. Roder, Evidence for barrier-limited protein folding kinetics on the microsecond time scale, Nat. Struct. Biol. 5 (1998) 385–392.
[20] A.C. Apetri, W.K. Surewicz, Kinetic intermediate in the folding of human prion protein, J. Biol. Chem. 277 (2002) 44589–44592.
[21] J.C. Lee, K.C. Engman, F.A. Tezcan, H.B. Gray, J.R. Winkler, Structural features of cytochrome c' folding intermediates revealed by fluorescence energy-transfer kinetics, Proc. Natl. Acad. Sci. USA 99 (2002) 14778–14782.
[22] B.A. Krantz, L. Mayne, J. Rumbley, S.W. Englander, T.R. Sosnick, Fast and slow intermediate accumulation and the initial barrier mechanism in protein folding, J. Mol. Biol. 324 (2002) 359–371.
[23] C.L. Jones, F. Fish, D.D. Muccio, Determination of RNase A/2′-cytidine monophosphate binding affinity and enthalpy by a global fit of thermal unfolding curves, Anal. Biochem. 302 (2002) 184–190.
[24] R.M. Ionescu, M.R. Eftink, Global analysis of the acid-induced and urea-induced unfolding of staphylococcal nuclease and two of its variants, Biochemistry 36 (1997) 1129–1140.
[25] A. Matouschek, J.M. Matthews, C.M. Johnson, A.R. Fersht, Extrapolation to water of kinetic and equilibrium data for the unfolding of barnase in urea solutions, Protein Eng. 7 (1994) 1089–1095.
[26] M.E. Zweifel, D. Barrick, Relationships between the temperature dependence of solvent denaturation and the denaturant dependence of protein stability curve, Biophys. Chem. 101–102 (2002) 221–237.
[27] G.S. Hammond, A correlation of reaction rates, J. Am. Chem. Soc. 77 (1955) 334–338.
[28] A. Bachmann, T. Kiefhaber, Apparent two-state tendamistat folding is a sequential process along a defined route, J. Mol. Biol. 306 (2001) 375–386.
[29] O. Bieri, T. Kiefhaber, Kinetic models in protein folding, in: R.H. Pain (Ed.), Mechanisms of Protein Folding, second ed., Oxford University Press, Oxford, UK, 2000, pp. 34–58.
[30] M. Silow, M. Oliveberg, High-energy channeling in protein folding, Biochemistry 36 (1997) 7633–7637.
[31] M. Oliveberg, Y.-J. Tan, M. Silow, A.R. Fersht, The changing nature of the protein folding transition state: implications for the shape of the free-energy profile for folding, J. Mol. Biol. 277 (1998) 933–943.
[32] G. Pappenberger, C. Saudane, M. Becker, A.E. Merbach, T. Kiefhaber, Denaturant-induced movement of the transition state of protein folding revealed by high-pressure stopped-flow measurements, Proc. Natl. Acad. Sci. USA 97 (2000) 17–22.